

UNIVERSITY OF BIRMINGHAM

Research at Birmingham

A level set based method for fixing overhangs in 3D printing

Cacace, Simone; Cristiani, Emiliano; Rocchi, Leonardo

DOI:

[10.1016/j.apm.2017.02.004](https://doi.org/10.1016/j.apm.2017.02.004)

License:

Creative Commons: Attribution-NonCommercial-NoDerivs (CC BY-NC-ND)

Document Version

Peer reviewed version

Citation for published version (Harvard):

Cacace, S, Cristiani, E & Rocchi, L 2017, 'A level set based method for fixing overhangs in 3D printing', Applied Mathematical Modelling. <https://doi.org/10.1016/j.apm.2017.02.004>

[Link to publication on Research at Birmingham portal](#)

General rights

Unless a licence is specified above, all rights (including copyright and moral rights) in this document are retained by the authors and/or the copyright holders. The express permission of the copyright holder must be obtained for any use of this material other than for purposes permitted by law.

- Users may freely distribute the URL that is used to identify this publication.
- Users may download and/or print one copy of the publication from the University of Birmingham research portal for the purpose of private study or non-commercial research.
- User may use extracts from the document in line with the concept of 'fair dealing' under the Copyright, Designs and Patents Act 1988 (?)
- Users may not further distribute the material nor use it for the purposes of commercial gain.

Where a licence is displayed above, please note the terms and conditions of the licence govern your use of this document.

When citing, please reference the published version.

Take down policy

While the University of Birmingham exercises care and attention in making items available there are rare occasions when an item has been uploaded in error or has been deemed to be commercially or otherwise sensitive.

If you believe that this is the case for this document, please contact UBIRA@lists.bham.ac.uk providing details and we will remove access to the work immediately and investigate.

Accepted Manuscript

A Level Set Based Method for Fixing Overhangs in 3D Printing

Simone Cacace, Emiliano Cristiani, Leonardo Rocchi

PII: S0307-904X(17)30100-2
DOI: [10.1016/j.apm.2017.02.004](https://doi.org/10.1016/j.apm.2017.02.004)
Reference: APM 11592

To appear in: *Applied Mathematical Modelling*

Received date: 11 January 2016
Revised date: 7 December 2016
Accepted date: 6 February 2017

Please cite this article as: Simone Cacace, Emiliano Cristiani, Leonardo Rocchi, A Level Set Based Method for Fixing Overhangs in 3D Printing, *Applied Mathematical Modelling* (2017), doi: [10.1016/j.apm.2017.02.004](https://doi.org/10.1016/j.apm.2017.02.004)



This is a PDF file of an unedited manuscript that has been accepted for publication. As a service to our customers we are providing this early version of the manuscript. The manuscript will undergo copyediting, typesetting, and review of the resulting proof before it is published in its final form. Please note that during the production process errors may be discovered which could affect the content, and all legal disclaimers that apply to the journal pertain.

Highlights

- A short review of math-oriented open problems in 3D printing is presented.
- A level-set method for fixing overhangs and avoiding support structures is proposed.
- The new method is particularly efficient if used with soluble filaments.

ACCEPTED MANUSCRIPT

A Level Set Based Method for Fixing Overhangs in 3D Printing

Simone Cacace^a, Emiliano Cristiani^b, Leonardo Rocchi^c

^a*Dipartimento di Matematica, Sapienza – Università di Roma, Rome, Italy*

^b*Istituto per le Applicazioni del Calcolo, Consiglio Nazionale delle Ricerche, Rome, Italy*
(corresponding author) *e.cristiani@iac.cnr.it*

^c*School of Mathematics, University of Birmingham, Birmingham, UK*

Abstract

3D printers based on the Additive Manufacturing technology create objects layer-by-layer dropping fused material. As a consequence, strong overhangs cannot be printed because the new-come material does not find a suitable support over the last deposited layer. In these cases, one can add support structures (scaffolds) which make the object printable, to be removed at the end. In this paper we propose a level set based method to create object-dependent support structures, specifically conceived to reduce both the amount of additional material and the printing time. We also review some open problems about 3D printing which can be of interests for the mathematical community.

Keywords: level set method, Hamilton-Jacobi equations, evolving interface, support structure, scaffolding, CAD software, additive manufacturing, fused deposition modelling, digital fabrication

2010 MSC: 65D17, 35F21

1. Introduction

2 Is a new industrial revolution coming? Many people think so: 3D printers
3 are able to create almost any solid object one can image and replicate existing
4 ones. Nowadays, the price of a 3D printer is small enough to allow many
5 people to have one at home, and create their own plastic objects. Within
6 a decade, some products may be downloaded from the Internet for printing
7 at home, causing a revolution in the market of such a small objects. Most
8 important, the number of printable materials is growing and it is already
9 possible printing an object mixing different materials. We leave to futurists

10 the comments about the time when 3D printers will be able to fully replicate
11 themselves.

12 While the computer science literature about 3D printing is already rich in
13 algorithms, optimization techniques and applications, the mathematical lit-
14 erature is basically null. This means that advanced mathematical tools based
15 on PDEs, optimal control theory and variational methods are, so far, little
16 explored. In order to fill the gap and promote the solution of the engineering
17 issues related to CAD 3D printer software, in the next section we propose a
18 bird-eye view over typical open problems encountered by practitioners who
19 use 3D printers based on Fused Decomposition Modeling (FDM).

20 *Main goal.* The core of the paper is devoted to the solution to a particular
21 problem, namely fixing the overhangs. When FDM technology is employed,
22 the solid object is created layer by layer, starting from the lowest one. As
23 a consequence, each layer can only be deposited *on top* of an existing sur-
24 face, otherwise the print material falls and solidifies “in the air”. In doing
25 this, little exceptions can be handled, i.e. the upper layer can protrude over
26 the lower layer within a certain limit. The more the material cools down
27 rapidly and the extruder moves slowly, the more the limit can be increased.
28 If the overhang exceeds the hardware limit, an additional support must be
29 necessarily added, in order to make the object printable. Note that the sup-
30 port structures are meant to be removed at the end of the process, and thus
31 they represent wasted material. Even more important, they represent an
32 additional source of printing time.

33 *Related work.* The overhang problem was already investigated in the com-
34 puter science and engineering literature, and some solutions were proposed
35 [1, 7, 11, 17, 19, 21]. In most cases, support structures fill either densely or
36 sparsely the free space encountered when a part is projected downward in
37 its build orientation, see left object in Fig. 1(b). The difference between the
38 methods is in how much material is used, the reliability of the supports, and
39 the type of material which can be used. The paper [1] proposes two support
40 geometry algorithms particularly suitable for weak support materials. The
41 paper [7] proposes an algorithm for the automatic generation of horizontal
42 bridges and vertical pillars, connected in such a way to create a hierarchical
43 structure. The paper [17] uses a cone-based scan to detect the closest points
44 which can serve as a support base (upon the model itself or the build plate)
45 for any overhanging point. The paper [11] uses instead slant hourglass-like
46 pillars. The paper [19] proposes to create cellular supports, riddling dense
47 structures with holes. The paper [21] proposes an algorithm which creates

48 thin tree-like hierarchical support structures, similar (but more efficient) to
49 the ones generated by the software Autodesk® Meshmixer® v2.9¹.

50 In this paper we propose to “enlarge” the object in such a way that
51 supports are no longer needed. In particular, we avoid the creation of pillars
52 which touch the build plate by means of optimally shaped chamfers, suitably
53 placed below hanging parts, see right object in Fig. 1(b).

54 2. What every mathematician should know about 3D printing

55 In the context of 3D printers there exist several open problems and mod-
56 elling needs. Generally speaking, the main issues come from the fact that
57 software solutions are not object-dependent, and not change during the print-
58 ing time, whereas each object (and each layer!) has its own peculiarities. An
59 exhaustive bibliography is out of the scope of the paper, therefore for each
60 problem we point out just a few significant references.

61 **Infill.** Printing fully solid objects is often not convenient because of the
62 large quantity of material to be used. Shape optimization tools can give the
63 optimal way to hollow out the object, reducing the overall material volume
64 and keeping at the same time the desired rigidity and printable features. The
65 problem reduces to finding the optimal inner structure supporting the whole
66 object from the inside [23] or partitioning the object to print hollow parts
67 [24].

68 **Orientation & supports.** In some cases the object is not 3D-printable
69 due to the presence of hanging parts. In this case one should find the orienta-
70 tion of the solid which minimizes the hanging parts [8] and then the minimal
71 amount of additional material needed to support the hanging parts. The
72 latter problem is the one we consider in this paper.

73 **Balancing.** It is important to ensure that during the printing process
74 (and once it is finished), the object can lie in equilibrium without falling
75 down. This problem can be solved by trying to balancing in an appropriate
76 way the mass of the object and by creating cavities in the inner structure
77 so that it stands in its natural pose without requiring any glue or pedestal
78 [4, 16].

79 **Partitioning.** Sometimes it is necessary to divide a 3D model into mul-
80 tiple printable pieces, so as to save the space, to reduce the printing time,

¹<http://www.meshmixer.com/>

81 or to make a large model printable by small printers. This problem was at-
82 tacked by means of a level set based approach similar to the one proposed
83 here in [25].

84 **Slicing & toolpath generation.** Creating layers from a 3D model is
85 a crucial step in 3D printing. Usually one computes the intersection curves
86 between the model represented by polygonal meshes and a sequence of paral-
87 lel planes. However, this procedure is not trivial in case of very complicated
88 (self-intersecting, overlapped) objects. Moreover, once the layers are created,
89 the exact trajectory of the nozzle must be defined. The infill pattern must
90 be travelled in the shortest way, continuously, without halting the manufac-
91 turing process, and minimizing the jump from the end of one sub-path to the
92 starting point of another sub-path. Interestingly, this problem can be seen
93 as a generalized travelling salesman problem [3, 6, 9, 10, 12].

94 **Shape or shading?** 3D-printed objects replicating real objects are usu-
95 ally made of a different (and cheaper) material with respect to the original
96 ones. As a consequence, it is expected that the replicated object reflects light
97 in a different manner (different albedo, different degree of Lambertianity),
98 thus resulting in an unsatisfactory product. In some cases it can be better
99 creating an object *with different shape but which appears as the original one*.
100 In other words, one aims at replicating the reflectance properties of an object,
101 not its original shape [13].

102 **Oozing.** It can happen that the machine deposits too much material in
103 some parts of the object, or the material oozes, especially when the nozzle
104 changes direction or stays on the same point for a long time. This issue is
105 mainly related to the temperature of the nozzle's hot end and the pressure
106 drop because of the filament. The nozzle's temperature, the retraction of
107 the filament and the speed of the extruder should be related to each other
108 and optimized with respect to the printing and travelling time (i.e. extruder
109 movements with and without emission of material, respectively).

110 **Multi-material printing.** Let us also mention the possibility to print
111 objects with different materials simultaneously, alternating them while print-
112 ing. Materials can have different reflectance properties and transparency,
113 and, consequently, endless combinations are possible, as well as related op-
114 timization processes. Similarly, one can coat the surface with paint, thus
115 altering the reflectance properties [22].

116 3. The level set method

117 The level set method was introduced in [15] and since then it was success-
 118 fully applied in many contexts, see e.g., [14, 18]. It allows to track Eulerianly
 119 the evolution of a $(d - 1)$ -dimensional surface embedded in \mathbb{R}^d transported
 120 by a given velocity vector field $\mathbf{v} : \mathbb{R}^d \rightarrow \mathbb{R}^d$. Let us briefly recall the method
 121 in the case of $d = 3$ which is of interest for our problem.

122 3.1. The level set function and the Hamilton–Jacobi equation

It is given a bounded closed surface $\Sigma_0 : U \subset \mathbb{R}^2 \rightarrow \mathbb{R}^3$ at initial time $t = 0$. We denote by Σ_t its (unknown) evolution under the action of \mathbf{v} at time t and by Ω_t the 3D domain strictly contained in Σ_t so that $\Sigma_t = \partial\Omega_t$, for all $t \geq 0$. The main idea of the level set method stems on the definition of a level set function $\varphi(t, x, y, z) : \mathbb{R}^+ \times \mathbb{R}^3 \rightarrow \mathbb{R}$ such that

$$\Sigma_t = \{(x, y, z) : \varphi(t, x, y, z) = 0\}, \quad \forall t \geq 0. \quad (1)$$

In this way the surface is recovered as the zero level set of φ at any time. Initially, the function φ is chosen in such a way that

$$\varphi(0, x, y, z) \begin{cases} > 0, & \text{if } (x, y, z) \notin \overline{\Omega}_0, \\ = 0, & \text{if } (x, y, z) \in \Sigma_0, \\ < 0, & \text{if } (x, y, z) \in \Omega_0. \end{cases} \quad (2)$$

A typical choice for $\varphi(0, x, y, z)$ is the signed distance function from Σ_0 , although this choice does not lead to a smooth function. It is easy to prove [18] that the level set function φ at any later time satisfies the following Hamilton–Jacobi equation

$$\partial_t \varphi + \mathbf{v} \cdot \nabla \varphi = 0, \quad t \in \mathbb{R}^+, (x, y, z) \in \mathbb{R}^3, \quad (3)$$

with a suitable initial condition $\varphi(0, x, y, z) = \varphi_0(x, y, z)$ satisfying (2). Here $\nabla = (\partial_x, \partial_y, \partial_z)$ denotes the gradient with respect to the space variables. One of the most appealing features of the level set method is that several geometrical properties of the evolving surface can be described by means of its level set function φ . For example, it is possible to write the unit exterior normal $\hat{\mathbf{n}}$ and the (mean) curvature κ in terms of φ and its derivatives. More precisely, we have

$$\hat{\mathbf{n}} = \frac{\nabla \varphi}{|\nabla \varphi|} \quad \text{and} \quad \kappa = \nabla \cdot \hat{\mathbf{n}}.$$

If the vector field has the form $\mathbf{v} = v\hat{\mathbf{n}}$ for some scalar function v , the equation (3) turns into

$$\partial_t \varphi + v|\nabla \varphi| = 0, \quad t \in \mathbb{R}^+, (x, y, z) \in \mathbb{R}^3. \quad (4)$$

123 3.2. Computation of the signed distance function

124 The computation of the signed distance function φ_0 is a problem *per se*.
 125 In our case, we can assume that the surface Σ_0 of the object to be printed
 126 is watertight and that it is given by means of a triangulation (typically in
 127 the form of a .STL file). Each triangle (facet) f is characterized by the 3D
 128 coordinates of its three vertices. Moreover, vertices are oriented in order to
 129 distinguish the internal and the external side of the facet (right-hand rule).

Given a point $(x, y, z) \in \mathbb{R}^3$, it is easy to find the distance $d((x, y, z), f)$ between the point and the facet, so that the unsigned distance from the surface is given by

$$d((x, y, z), \Sigma_0) = \min_f d((x, y, z), f).$$

130 The computation of the distance's sign is more tricky since one has to check
 131 if the point is internal or external to the surface. Several methods can be
 132 employed here. For example, one can note that the solid angle subtended by
 133 the whole surface at a given point is maximal and equal to 4π iff the point is
 134 internal. Then, one can sum all the solid angles subtended by the facets at
 135 the point and check if it equals 4π . If this is the case, the point is internal
 136 to the surface, otherwise it is external.

137 Note that the solid angle itself should be *signed*, in the sense that it
 138 must be positive if the point looks at the internal part of the facet, negative
 139 otherwise. A nice algorithm to compute the signed solid angle between a
 140 point and a triangle was given by van Oosterom and Strackee [20].

141 4. Fixing overhangs

142 In this section we propose a solution for fixing the overhang issue in 3D
 143 printing and, in most cases, getting rid of long support structures extended
 144 until the build plate. We want to use the level set method by considering the
 145 domain Ω as the object to be printed and its surface Σ as an evolving front.
 146 Therefore, the idea is to modify the initial unprintable object Ω_0 letting it
 147 evolve by an *ad hoc* vector field \mathbf{v} until it becomes fully printable, meaning

148 that there are no more unprintable hanging parts. The final object Ω_* is
 149 then actually printed and the difference $\Omega_* \setminus \Omega_0$ is finally removed. Note that
 150 the difference $\Omega_* \setminus \Omega_0$ can be easily identified by standard techniques and
 151 consequently printed with a different material (e.g., a soluble filament) or
 152 with a different printing resolution.

It is useful to divide the surface Σ of the object Ω in three subsets, on
 the basis of their *printability*. To this end, we denote by $\hat{\mathbf{g}} = (0, 0, -1)$ the
 unit gravity vector, and again by $\hat{\mathbf{n}}(x, y, z)$ the exterior unit normal to the
 surface Σ of the object Ω at the point (x, y, z) . Moreover, let

$$\theta(\hat{\mathbf{n}}) := \arccos(\hat{\mathbf{g}} \cdot \hat{\mathbf{n}}) \quad (5)$$

153 be the angle between $\hat{\mathbf{g}}$ and $\hat{\mathbf{n}}$.

154 **Definition 4.1.** A point (x, y, z) of the surface Σ is said to be

$$\begin{aligned} & \text{unprintable,} && \text{if } \theta \in [0, \bar{\alpha}] \cup (2\pi - \bar{\alpha}, 2\pi], \\ & \text{safe,} && \text{if } \theta \in [\pi/2, 3\pi/2], \\ & \text{modifiable,} && \text{otherwise,} \end{aligned}$$

156 where $\bar{\alpha}$ is a given limit angle², see Fig. 1(a).

157 While the first two definitions are immediately clear, it is worth to spend
 158 some words on the third one. Modifiable points are indeed printable since
 159 the overhang is sufficiently small. On the other hand, it could be convenient
 160 to move those points as well in order to make printable the unprintable ones.
 161 This guarantees a sufficient flexibility to shape the object conveniently and
 162 not to create long supports like the one depicted on the left of Fig. 1(b). We
 163 can extend Definition 4.1 by saying that the set of both modifiable and safe
 164 point constitute the overall printable points.

165 The rest of the section will be devoted to the construction of the vector
 166 field \mathbf{v} . A suitable choice is the one used in equation (4) where $\mathbf{v} = v\hat{\mathbf{n}}$ for
 167 some scalar function v , possibly depending on $\hat{\mathbf{n}}$ and κ .

In the following we denote by

$$P(\omega) := \omega^+ \quad \text{and} \quad M(\omega) := \omega^-, \quad \omega \in \mathbb{R},$$

²Typically $\bar{\alpha} = \frac{\pi}{4}$, because of the so-called 45 degree rule, though it actually depends
 on the 3D printer settings, print material, cooling, etc.

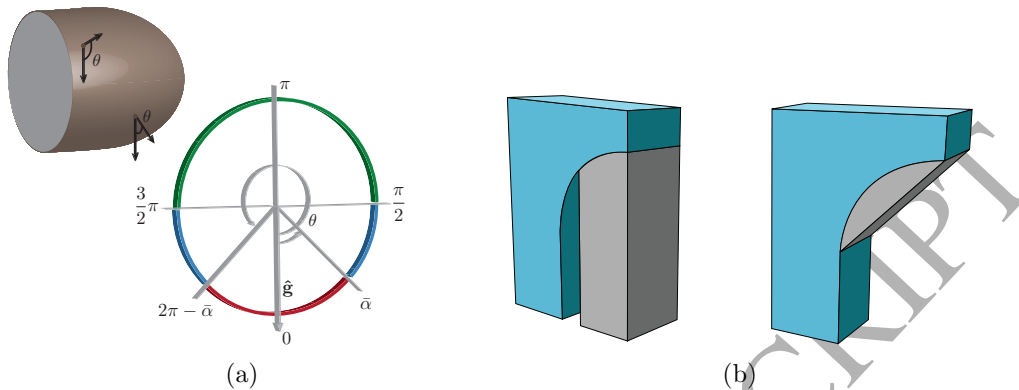


Figure 1: (a) Unprintable (red), modifiable (blue) and safe (green) points with respect to the counter-clockwise angle θ between the gravity $\hat{\mathbf{g}}$ and the normal $\hat{\mathbf{n}}$. Modifiable and safe points are printable. (b) The left grey support wastes a lot of material contrary to the chamfer on the right that saves more material and keeps the printability of the overhang as well.

168 the positive and negative part, respectively.

169 **Positivity and build plate.** We need to be guaranteed that $\Omega_0 \subseteq \Omega_t \subseteq \Omega_*$,
 170 for all $t \geq 0$, since once the object is printed we can remove material but not
 171 add new one. This is why we need $v \geq 0$, i.e. the movement of each point of
 172 the surface Σ has to be along the normal exterior direction $\hat{\mathbf{n}}$. Furthermore,
 173 the object cannot move under the build plate, supposed at a fixed $z = z_{\min} \in$
 174 \mathbb{R} . Then we impose $v = 0$ if $z \leq z_{\min}$.

Movement of unprintable points. We introduce the term

$$v_1(\hat{\mathbf{n}}; \bar{\alpha}) := P(\cos \theta(\hat{\mathbf{n}}) - \cos \bar{\alpha}), \quad (6)$$

175 which lets the unprintable points move outward. The speed is higher when-
 176 ever θ is close to 0, which represents the (hardest) case of a horizontal hanging
 177 part.

178 **Rotation.** It is convenient introducing a rotational effect in the evolution
 179 which avoids the unprintable regions to evolve “as it is” until they touch the
 180 build plate. To this end we introduce the term $(z_{\max} - z)$, where $z_{\max} \in \mathbb{R}$
 181 is the maximal height reached by the object. This term simply increases the
 182 speed of lower points with respect to higher ones. This makes the lower parts
 183 be resolved (or eventually touch the built plate) before the higher parts, thus
 184 saving material.

Movement of modifiable points. Modifiable points are moved, if necessary, by means of the following term in the vector field

$$v_2(\kappa) := M(\kappa). \quad (7)$$

185 It moves outward the points with negative curvature until it vanishes, i.e.
186 the surface is locally flat. In particular, it moves concave corners and let
187 modifiable points become a suitable support for the still unprintable points
188 above.

189 **Blockage of safe points.** Finally, it is necessary to exclude from the evolu-
190 tion the safe points of the object. In order to identify them, we use the sign
191 of the third component n_3 of the unit exterior normal vector $\hat{\mathbf{n}}$.

By putting together all the terms we end up with

$$v(x, y, z, \hat{\mathbf{n}}, \kappa; \bar{\alpha}) := \begin{cases} C_1 (z_{\max} - z)v_1(\hat{\mathbf{n}}; \bar{\alpha}) + C_2 v_2(\kappa), & \text{if } n_3 < 0 \text{ and } z > z_{\min}, \\ 0, & \text{otherwise,} \end{cases} \quad (8)$$

192 with $C_1, C_2 > 0$ positive constants (model parameters). The result expected
193 from a such vector field is an evolution similar to the one depicted on the
194 right in Fig. 1(b), corresponding to a support whereby the angle θ in each of
195 its point is less or equal to $\bar{\alpha}$.

196 The surface evolution relative to equation (4) must be stopped at some
197 final time $T > 0$. Rather than waiting that the velocity field vanishes com-
198 pletely, it is convenient to check directly (at every time $t < T$) whether the
199 overall surface is printable or not, according to Definition 4.1. More precisely,
200 we stop the evolution when all the points belonging to the zero level set are
201 safe or modifiable, i.e., printable.

202 **Remark 4.1.** (Optimality of the final surface) By construction, the surface
203 always evolves towards a printable object. Indeed, any non-printable part
204 of the surface is forced to move downward, and the surface has to stop once
205 the build plate is reached. Nevertheless, we have no guarantee that the final
206 object is “optimal” in terms of additional printing material. In the worst-
207 case scenario the surface evolves until it touches the build plate, obtaining
208 something similar to the results depicted on the left in Fig. 1(b). For in-
209 stance, this is the case of a perfectly symmetric bridge-shaped object, unless
210 some symmetry-breaking terms are added in the evolution model. Likely, the
211 method works fine in most cases, as one can see in section 6, where several
212 objects are tested.

213 **5. Theoretical analysis**

214 In this section we show that a slightly regularised version of the Hamilton–
 215 Jacobi equation (4) with velocity field (8) fits the classical theory of viscosity
 216 solutions and it is then well-posed.

Consider a general second order PDE of the form

$$\varphi_t + F(t, \mathbf{x}, \varphi, \nabla\varphi, \mathbf{H}\varphi) = 0, \quad t > 0, \quad \mathbf{x} \in \mathbb{R}^n, \quad (9)$$

where $\mathbf{H}\varphi$ is the Hessian matrix of φ and $F : \mathbb{R}^+ \times \mathbb{R}^n \times \mathbb{R} \times \mathbb{R}^n \times \mathcal{S}_n \rightarrow \mathbb{R}$ is continuous and \mathcal{S}_n is the set of symmetric $n \times n$ matrices. Resorting to classical results [5], we can say that the IVP for (9) is well-posed if the function F is *proper* for any fixed $t \in [0, T]$, i.e.

$$\forall t \quad F(t, \mathbf{x}, r, \mathbf{p}, \mathbf{X}) \leq F(t, \mathbf{x}, s, \mathbf{p}, \mathbf{Y}) \quad \text{whenever } r \leq s \text{ and } \mathbf{Y} \leq \mathbf{X}. \quad (10)$$

217 Before writing our equation in the form (9), let us note that $M(\omega) = P(-\omega)$
 218 for all $\omega \in \mathbb{R}$, and $M(c\omega) = cM(\omega)$, for all $\omega \in \mathbb{R}$ and $c > 0$. Moreover, let
 219 $H : \mathbb{R} \rightarrow \{0, 1\}$ be the Heaviside function and state the following equality:

Lemma 5.1. Given any function $u \in C^2(\mathbb{R}^n; \mathbb{R})$, we have

$$\operatorname{div} \left(\frac{\nabla u}{|\nabla u|} \right) |\nabla u| = \operatorname{trace} \left(\left(\mathbf{I} - \frac{\nabla u \otimes \nabla u}{|\nabla u|^2} \right) \mathbf{H}u \right),$$

220 where \mathbf{I} is the $n \times n$ identity matrix and $(\mathbf{a} \otimes \mathbf{b})_{i,j} = a_i b_j$ for all $\mathbf{a}, \mathbf{b} \in \mathbb{R}^n$
 221 and $i, j = 1, \dots, n$.

222 The proof of the Lemma is postponed in the Appendix.

Making explicit the dependence on φ , we can rewrite the speed as

$$v(z, \nabla\varphi, \mathbf{H}\varphi; \bar{\alpha}) = \left[C_1(z_{\max} - z)M \left(\frac{\partial_z \varphi}{|\nabla\varphi|} + \cos \bar{\alpha} \right) + C_2M \left(\operatorname{div} \left(\frac{\nabla\varphi}{|\nabla\varphi|} \right) \right) \right] H(-\partial_z \varphi) H(z - z_{\min}).$$

Note that in our case the function v does not depend explicitly on t and φ , but depends implicitly on $\mathbf{H}\varphi$ by means of the divergence operator. In our

case we have $F = v|\nabla\varphi|$, and then, using Lemma 5.1, we have

$$\begin{aligned}
F(z, \nabla\varphi, \mathbf{H}\varphi; \bar{\alpha}) = & \\
& \left[C_1(z_{\max} - z)M(\partial_z\varphi + |\nabla\varphi|\cos\bar{\alpha}) + \right. \\
& \left. C_2M\left(\operatorname{div}\left(\frac{\nabla\varphi}{|\nabla\varphi|}\right)|\nabla\varphi|\right) \right] H(-\partial_z\varphi)H(z - z_{\min}) = \\
& \left[C_1(z_{\max} - z)M(\partial_z\varphi + |\nabla\varphi|\cos\bar{\alpha}) + \right. \\
& \left. C_2M\left(\operatorname{trace}\left(\left(\mathbf{I} - \frac{\nabla\varphi \otimes \nabla\varphi}{|\nabla\varphi|^2}\right)\mathbf{H}\varphi\right)\right) \right] H(-\partial_z\varphi)H(z - z_{\min}).
\end{aligned}$$

Following again [5] (Example 1.2), and considering the sign of the function M , we are left to prove that the matrix $\left(\mathbf{I} - \frac{\mathbf{p} \otimes \mathbf{p}}{|\mathbf{p}|^2}\right)$, $\mathbf{p} \in \mathbb{R}^3$, is positive semi-definite. A straightforward computation shows that, for all vectors $(x_1, x_2, x_3) \neq (0, 0, 0)$,

$$\begin{aligned}
(x_1 \ x_2 \ x_3) \left(\mathbf{I} - \frac{\mathbf{p} \otimes \mathbf{p}}{|\mathbf{p}|^2}\right) \begin{pmatrix} x_1 \\ x_2 \\ x_3 \end{pmatrix} = \\
\frac{1}{|\mathbf{p}|} [(x_1p_2 - x_2p_1)^2 + (x_1p_3 - x_3p_1)^2 + (x_2p_3 - x_3p_2)^2] \geq 0.
\end{aligned}$$

223 This proves that F is proper. In order to entirely fit the theoretical frame-
224 work we should guarantee the continuity of the function F , although this is
225 not expected to be a crucial point from the numerical point of view, since
226 continuity cannot be actually satisfied a discrete level. An easy solution is
227 the mollification of the Heaviside function by convolution, which makes F be
228 continuous.

229 6. Numerical tests

230 We solve equation (4) with velocity (8) by using a monotone upwind
231 scheme based on finite differences as described in [18, Sect. 6.4], with an
232 adaptive time step in order to strictly satisfy the CFL condition.

233 As a preliminary test, we solved a dimension-reduced problem by con-
 234 sidering a 2D interface Σ with two hanging parts as the zero level set of a
 235 specific level set function $\varphi : \mathbb{R}^+ \times \mathbb{R}^2 \rightarrow \mathbb{R}$. The computational domain is
 236 $[0, 6] \times [0, 10]$, divided in 120×200 regular grid nodes. Parameters are $C_1 = 6$
 237 and $C_2 = 0.4$. Initial and final shapes of the interface are shown in Fig. 2(a).
 238 Moreover, by “extruding” the 2D domain Ω , as it was a section of a real 3D
 239 object, we printed it out with the supports created from our method (Fig.
 240 2(b)), and keeping the scaffolding structure created by the commercial soft-
 241 ware Cura v15.04.2 (Fig. 2(c)). Finally, Fig. 2(d) shows the support structure
 generated by the commercial software Autodesk® Meshmixer® v2.9.

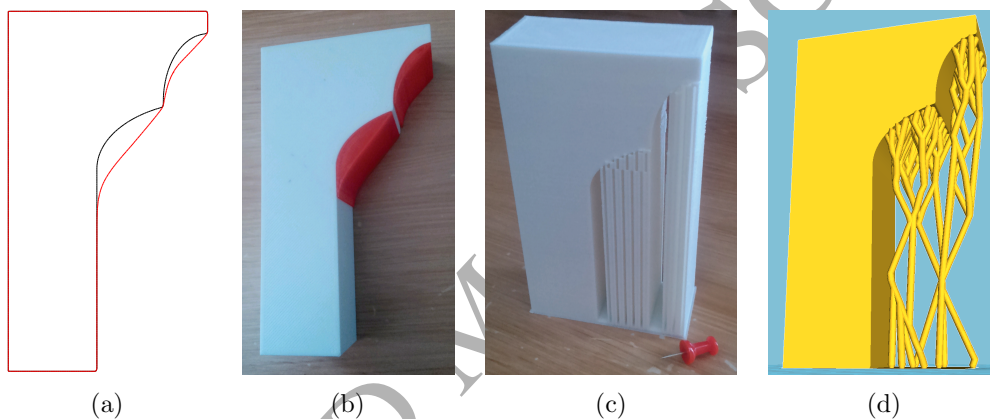


Figure 2: 2D test. (a) Initial contour Σ_0 (black) and the optimized one Σ_* (red) after the evolution. (b) Printed model with proposed support. (c) Printed model with support structure generated by free software Cura v15.04.2. (d) Tree-like support structure generated by Autodesk® Meshmixer® v2.9.

242 Moving to real 3D problems, we tested eight objects. In all cases the
 243 computational domain $[-2, 2]^3$ is divided in 100^3 regular grid nodes. The
 244 first two examples, a sphere and a cross, are shown in Fig. 3(a,b). They have
 245 been easily obtained as the zero level set of a corresponding hyper-surface
 246 embedded in \mathbb{R}^4 and no .STL files have been required. The parameters used
 247 for the evolution are $C_1 = 0.7$, $C_2 = 0.3$ for the sphere and $C_1 = 1.5$, $C_2 = 0.5$
 248 for the cross.
 249

250 These simple numerical tests clearly show the advantage of the proposed
 251 approach: the additional material used to make the object printable is rather
 252 minimal, being concentrated in the critical zones. No evident waste of materi-
 253 al is visible. More precisely, we see that the additional material is limited

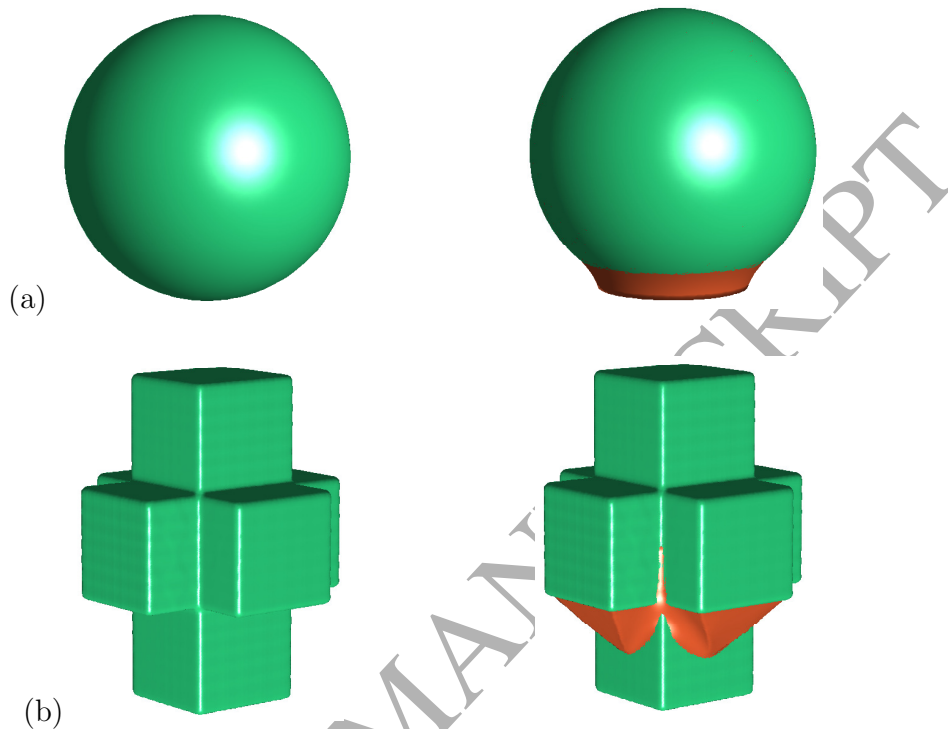


Figure 3: Two simple objects. Initial surface (left) and final result (right).

254 to the quantity needed to support overhangs within the maximum allowed
 255 slope.

256 The following three examples are shown in Fig. 4(a,b,c). In this case, we
 257 obtained the objects as the zero level set of the distance function (see section
 258 3.2) for the corresponding surface given as .STL file. The parameters used
 259 for the evolution are (a) $C_1 = 0.8$, $C_2 = 0.8$, (b) $C_1 = 1.8$, $C_2 = 0.6$, and (c)
 260 $C_1 = 0.6$, $C_2 = 1.2$.

261 Again we see that the additional material is rather minimal and concen-
 262 trated in the critical zones.

263 The last three examples are shown in Fig. 5(a,b,c). In this case we tried
 264 to fix overhangs of some mechanical components, starting again from the
 265 corresponding .STL files. The parameters used for the evolution are (a)
 266 $C_1 = 3.5$, $C_2 = 0.9$, (b) $C_1 = 1.2$, $C_2 = 1.6$, and (c) $C_1 = 5.6$, $C_2 = 0.3$.

267 In the first two cases the evolution is close to the optimal one since no
 268 evident waste of material is visible. In the last case instead, the horizontal

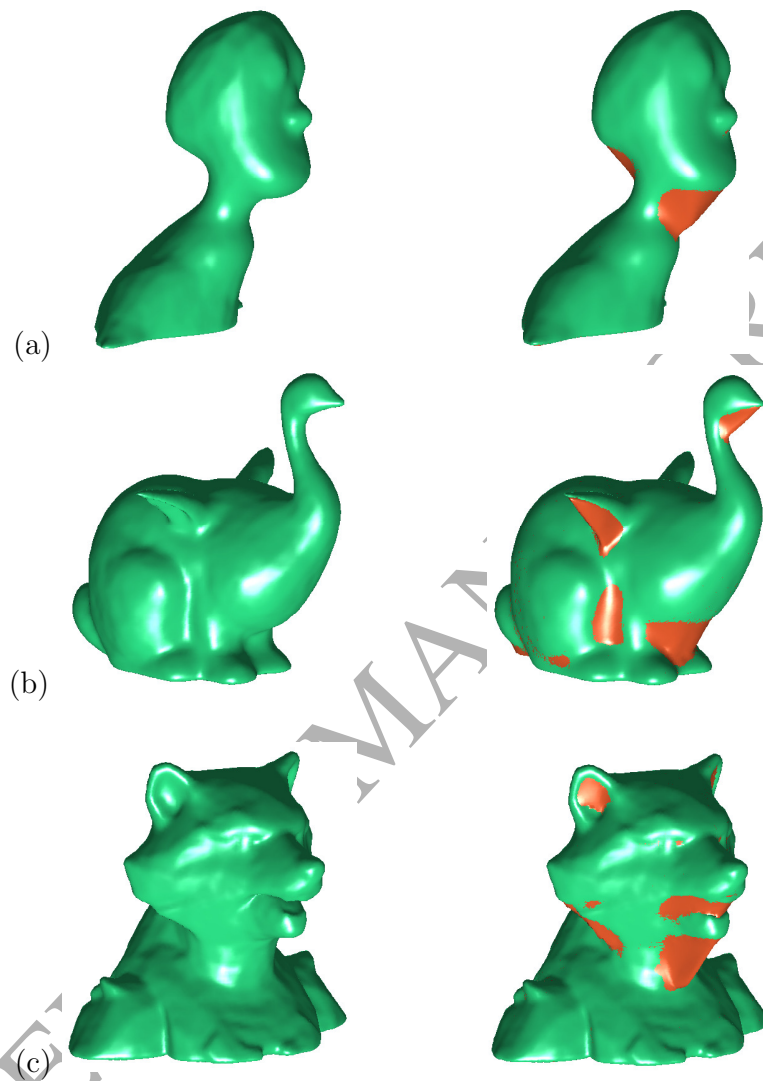


Figure 4: Three objects. Initial surface (left) and final result (right).

269 holes on the overhanging part are a challenge for the proposed method. They
270 hinder the rotation and make the surface evolve vertically until the build plate
271 is reached, thus realizing the worst-case scenario discussed in Remark 4.1.

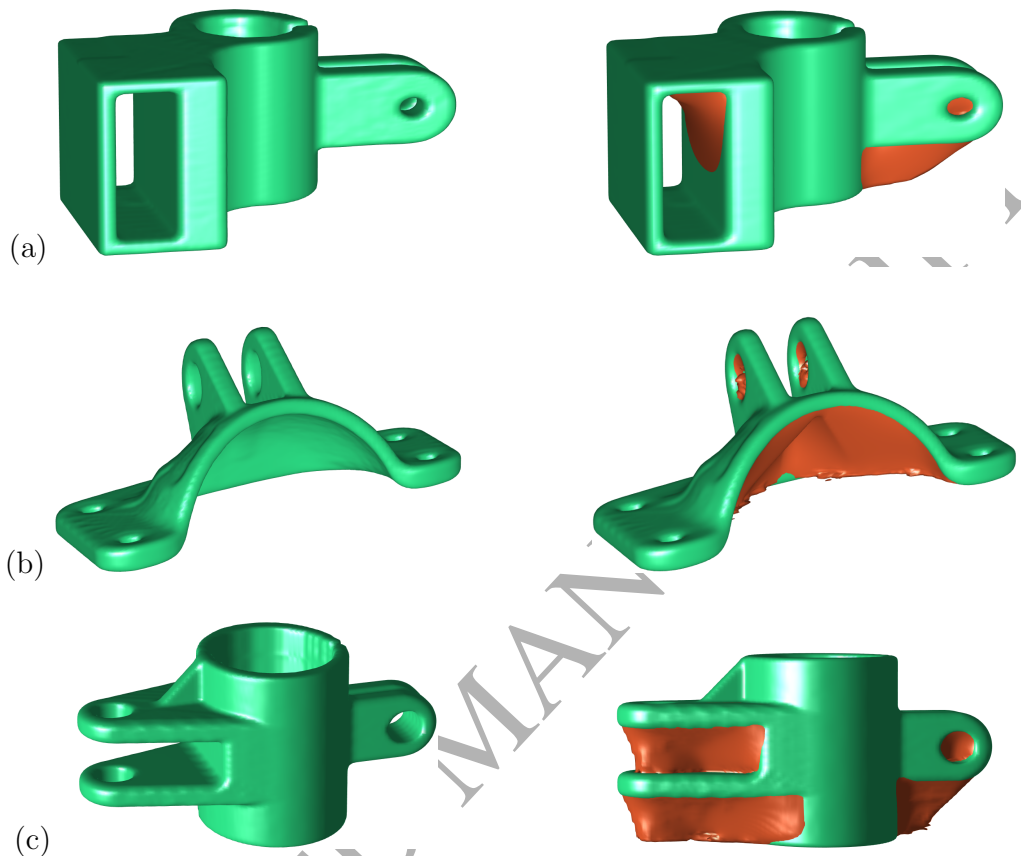


Figure 5: Three brackets. Initial surface (left) and final result (right).

272 Conclusions and future work

273 We have introduced a level set based method to create *ad hoc* chamfers
 274 in additive manufacturing, avoiding in most cases the use of classical vertical
 275 support structures. Moreover, in the worst-case scenario the evolved surface
 276 will not be worse than the one obtained with commercial software.

277 The main drawback of the proposed approach is that objects with small
 278 or sharp details clearly require a quite fine computational grid, thus rising
 279 the CPU time. Note that this is not a limitation of the evolution model,
 280 rather a limitation of the level set method itself.

281 Let us also stress here that we consider only the overhanging issue in
 282 printability, although the use of the support structure is not just for over-
 283 hangs. As recalled in section 2, it also keeps the whole model from falling

284 because of the gravity. Moreover, for printers that use the same material for
 285 both the model and the support structure, removing the support structure
 286 from the model can become difficult too. For all these reasons the proposed
 287 method is more suitable for printers that use different materials for the sup-
 288 port structure, such as polyjet printers.

289 We hope that this study can pave the way to shape optimization methods
 290 based on the coupling of the level set method and the shape derivatives [2].
 291 In that context one could minimize directly the printing time and at the same
 292 time penalize the contact between the desired object and the removable parts,
 293 in order to simplify the final detaching operations.

294 Acknowledgements

295 Authors want to thank Maurizio Falcone for the useful discussions about
 296 the model developed in this paper.

297 Appendix A. Proof of Lemma 5.1

Proof. First of all, it is useful to recall a basic property of the trace operator.
 Let us consider two $n \times n$ matrices \mathbf{A} and \mathbf{B} , and define $\mathbf{C} := \mathbf{AB}$. Denote
 by $\mathbf{a}_{i,\cdot}$ the i -th row of \mathbf{A} and by $\mathbf{b}_{\cdot,j}$ the j -th column of \mathbf{B} . We have

$$\text{trace}(\mathbf{C}) \stackrel{\text{def}}{=} \sum_i c_{i,i} = \sum_i \mathbf{a}_{i,\cdot} \cdot \mathbf{b}_{\cdot,i} = \sum_i \sum_j a_{i,j} b_{j,i}. \quad (\text{A.1})$$

The Lemma is proved as follows:

$$\begin{aligned}
|\nabla u| \operatorname{div} \left(\frac{\nabla u}{|\nabla u|} \right) &= |\nabla u| \sum_{i=1}^n \partial_i \left(\frac{\partial_i u}{|\nabla u|} \right) = \\
|\nabla u| \frac{1}{|\nabla u|^2} \sum_{i=1}^n \left(\partial_i^2 u |\nabla u| - \partial_i u \frac{1}{|\nabla u|} \sum_{j=1}^n \partial_j u \partial_i \partial_j u \right) &= \\
\Delta u - \frac{1}{|\nabla u|^2} \sum_{i=1}^n \partial_i u \sum_{j=1}^n \partial_j u \partial_i \partial_j u &= \\
\Delta u - \frac{1}{|\nabla u|^2} \sum_{i=1}^n \sum_{j=1}^n (\nabla u \otimes \nabla u)_{i,j} \partial_i \partial_j u &= \\
\operatorname{trace}(\mathbf{H}u) - \sum_{i=1}^n \sum_{j=1}^n \frac{(\nabla u \otimes \nabla u)_{i,j}}{|\nabla u|^2} \partial_j \partial_i u &\stackrel{(A.1)}{=} \\
\operatorname{trace}(\mathbf{H}u) - \operatorname{trace} \left(\frac{\nabla u \otimes \nabla u}{|\nabla u|^2} \mathbf{H}u \right) &= \\
\operatorname{trace} \left(\left(I - \frac{\nabla u \otimes \nabla u}{|\nabla u|^2} \right) \mathbf{H}u \right). &\quad \square
\end{aligned}$$

References

- [1] E. Barnett and C. Gosselin. Weak support material techniques for alternative additive manufacturing materials. *Additive Manufacturing*, 8:95–104, 2015.
- [2] M. Burger and S. J. Osher. A survey on level set methods for inverse problems and optimal design. *Eur. J. Appl. Math.*, pages 263–301, 2005.
- [3] K. Castelino, R. D’Souza, and P. K. Wright. Toolpath optimization for minimizing airtime during machining. *Journal of Manufacturing Systems*, 22(3):173–180, 2003.
- [4] A. N. Christiansen, R. Schmidt, and J. A. Bærentzen. Automatic balancing of 3D models. *Computer-Aided Design*, 58:236–241, 2015.
- [5] M. G. Crandall, H. Ishii, and P.-L. Lions. User’s guide to viscosity solutions of second order partial differential equations. *Bull. Amer. Math. Soc.*, 27(1):1–67, 1992.

- 312 [6] S. Dhanik and P. Xirouchakis. Contour parallel milling tool path gen-
313 eration for arbitrary pocket shape using a fast marching method. *Int.*
314 *J. Adv. Manuf. Technol.*, 50(9-12):1101–1111, 2010.
- 315 [7] J. Dumas, J. Hergel, and S. Lefebvre. Bridging the gap: automated
316 steady scaffoldings for 3D printing. *ACM Trans. Graph.*, 33(4):Article
317 No.98(10 pages), 2014.
- 318 [8] B. Ezair, F. Massarwi, and G. Elber. Orientation analysis of 3D objects
319 toward minimal support volume in 3D-printing. *Computers & Graphics*,
320 51:117–124, 2015.
- 321 [9] K. Hildebrand, B. Bickel, and M. Alexa. Orthogonal slicing for additive
322 manufacturing. *Computers & Graphics*, 37(6):669–675, 2013.
- 323 [10] P. Huang, C. C. L. Wang, and Y. Chen. Intersection-free and topo-
324 logically faithful slicing of implicit solid. *J. Comput. Inf. Sci. Eng.*,
325 13(2):021009, 2013.
- 326 [11] X. Huang, C. Ye, S. Wu, K. Guo, and J. Mo. Sloping wall structure
327 support generation for fused deposition modeling. *Int. J. Adv. Manuf.*
328 *Technol.*, 42:1074–1081, 2009.
- 329 [12] Y.-A. Jin, Y. He, J.-Z. Fu, W.-F. Gan, and Z.-W. Lin. Optimization of
330 tool-path generation for material extrusion-based additive manufactur-
331 ing technology. *Additive Manufacturing*, 1-4:32–47, 2014.
- 332 [13] Y. Lan, Y. Dong, F. Pellacini, and X. Tong. Bi-scale appearance fabri-
333 cation. *ACM Trans. Graph.*, 32(4):Article No.145(12 pages), 2013.
- 334 [14] S. Osher and R. Fedkiw. *Level set methods and dynamic implicit sur-*
335 *faces*, volume 153 of *Applied Mathematical Sciences*. Springer-Verlag,
336 New York, 2003.
- 337 [15] S. Osher and J. A. Sethian. Front propagating with curvature-dependent
338 speed: algorithms based on Hamilton-Jacobi formulations. *J. Comput.*
339 *Phys.*, 79(1):12–49, 1988.
- 340 [16] R. Prévost, E. Whiting, S. Lefebvre, and O. Sorkine-Hornung. Make
341 it stand: balancing shapes for 3D fabrication. *ACM Trans. Graph.*,
342 32(4):Article No.81(10 pages), 2013.

- 343 [17] J. Qiu, L. Wu, and Y. Mao. A novel supporting structure generation
344 scheme to 3D printing. In *Proceedings of the 7th International Confer-*
345 *ence on Internet Multimedia Computing and Service*, ICIMCS '15, pages
346 69:1–69:4, New York, NY, USA, 2015. ACM.
- 347 [18] J. A. Sethian. *Level set methods and fast marching methods: evolving*
348 *interfaces in computational geometry, fluid mechanics, computer vision,*
349 *and material science*. Cambridge University Press, New York, 1999.
- 350 [19] G. Strano, L. Hao, R. M. Everson, and K. E. Evans. A new approach
351 to the design and optimisation of support structures in additive manu-
352 facturing. *Int. J. Adv. Manuf. Technol.*, 66:1247–1254, 2013.
- 353 [20] A. van Oosterom and J. Strackee. The solid angle of a plane trian-
354 gle. *IEEE Transactions on Biomedical Engineering*, BME-30(2):125–
355 126, 1983.
- 356 [21] J. Vanek, J. A. G. Galicia, and B. Benes. Clever support: efficient
357 support structure generation for digital fabrication. *Comput. Graph.*
358 *Forum*, 33(5):117–125, 2014.
- 359 [22] K. Vidimče, S.-P. Wang, J. Ragan-Kelley, and W. Matusik. OpenFab:
360 a programmable pipeline for multi-material fabrication. *ACM Trans.*
361 *Graph.*, 32(4):Article No.136(12 pages), 2013.
- 362 [23] W. Wang, T. Y. Wang, Z. Yang, L. Liu, X. Tong, W. Tong, J. Deng,
363 F. Chen, and X. Liu. Cost-effective printing of 3D objects with skin-
364 frame structures. *ACM Trans. Graph.*, 32(6):Article No.177(10 pages),
365 2013.
- 366 [24] X.-R. Wei, Y.-H. Zhang, and G.-H. Geng. No-infill 3d printing. *3D Res.*,
367 7(24), 2016.
- 368 [25] M. Yao, Z. Chen, L. Luo, R. Wang, and H. Wang. Level-set-based
369 partitioning and packing optimization of a printable model. *ACM Trans.*
370 *Graph.*, 34(6):Article No.214(11 pages), 2015.